Application of admittance optimization to the design of a low-height tramway noise barrier

Alexandre Jolibois[a)]
Denis Duhamel[b)]
Université Paris-Est, Laboratoire Navier, ENPC-IFSTTAR-CNRS, UMR 8205
Ecole des Ponts ParisTech, 6 & 8 av. Blaise Pascal
Champs-sur-Marne, 77455 Marne La Vallée Cedex 2, France

Victor W. Sparrow[c)]
Graduate Program in Acoustics, The Pennsylvania State University
201 Applied Science Building, University Park, 16802, USA

Jérôme Defrance[d)]
Philippe Jean[e)]
Centre Scientifique et Technique du Bâtiment
24, rue Joseph Fourier, 38400 Saint Martin d'Hères, France

An urban low-height barrier meant to attenuate tramway noise emission for nearby walking pedestrians or cyclists is studied. A numerical method coupling the two dimensional BEM and a gradient-based optimization algorithm is proposed to optimize the admittance distribution on the barrier in order to enhance the broadband insertion loss in the shadowing zone. The gradient of the broadband attenuation is calculated efficiently using the adjoint state approach which makes it possible to use a large number of parameters without significant increase of computation time and to consider a barrier of arbitrary shape. A few admittance designs coupling porous layers and micro-perforated resonant panels covering barriers of classical shapes are proposed, all showing an improvement of several dB(A) compared to more simple admittance distributions.

[a)]email: alexandre.jolibois@enpc.fr
[b)]email: denis.duhamel@enpc.fr
[c)]email: vws1@psu.edu
[d)]email: jerome.defrance@cstb.fr
[e)]email: philippe.jean@cstb.fr

1 INTRODUCTION

In the past forty years, there has been a lot of effort in trying to design more efficient noise barriers, especially for highways. However, there is an increasing concern in reducing noise exposure not only close to highways but also in urban areas[1–5]. Because the propagation distances are small, near field interference effects are expected to be stronger than in the highway case, and those effects will depend greatly on the shape and the surface admittance (the reciprocal of the impedance). Optimization of the surface impedance coverage to maximize the attenuation is therefore likely to be efficient[4,5].

As an example application, in this paper we consider a low-height (one meter high) barrier of arbitrary shape meant to attenuate tramway noise and we allow the surface admittance to be optimized by an iterative optimization method. A recent study[6] showed that most of the noise emitted by a modern tramway comes from sources close to the ground and therefore a low height barrier could provide a significant attenuation. The attenuation and its gradient are calculated efficiently using the boundary element method (BEM) and the adjoint state approach[7]. With this method, the gradient is expressed as a post-treatment of the BEM and therefore its calculation does not require coding a new solver and can even be achieved using results from any commercial BEM software. Besides, the choice of a gradient-based optimization method as opposed to an evolutionary method has been made to take advantage of the gradient information which can be easily obtained in this context.

We first present the barrier implementation and the objective function to minimize. Then the calculation of the functional gradient with respect to the admittance based on the adjoint state is derived. Finally, the gradient calculation is used in a classical optimization method in order to design the admittance distribution of a low-height tramway noise barrier of different geometries.

2 BARRIER IMPLEMENTATION AND MODELING

2.1 Physical assumptions and geometry

The atmosphere is assumed homogeneous with a speed of sound of $c_0 = 343\,\mathrm{m/s}$. Pallas et al. showed[6] that most of the noise emitted by a modern tramway rolling at 40 km/h on rigid paving comes from three sources close to the ground: rail track, powered and un-powered bogie. We model those sources as one infinite, omni-directional line source lying on the ground, with a spectral content given by the incoherent sum of the three identified sources (see Fig. 2). One can infer that most of the A-weighted acoustic energy is contained in the frequency range 100-5000 Hz. However we will constrain the frequency range to 100-2500 Hz which is a good compromise between the accuracy of the broadband insertion loss and computation time. It is also assumed that the geometry is invariant along the axis of the track, which makes the problem purely two dimensional. This assumption has been shown[8] to be correct when predicting excess attenuation at single frequencies due to point sources, which is what we will use in the calculation of the broadband insertion loss.

The presence of the tramway will cause the sound to bounce on its surface and diffract at the roof edge and at the gap between the carriage and the ground. Those geometrical details could be modeled with the BEM, but as a first approximation, one can model the tramway side as an infinite rigid vertical baffle (see in Fig. 1). This idealization is equivalent to introducing an *image* barrier, symmetrical to the original one with respect to the tramway side surface, and therefore the meshed surface is greatly reduced with this approximation. Finally, the ground is modeled as rigid, which represents correctly many urban-like surfaces.

The barrier cross section is assumed to lie in a one meter wide square, half a meter away from the tramway (see Fig. 1). The receiver locations have been chosen to represent a range of possible locations of pedestrian ears: horizontal distance from the bottom-right corner of the barrier between 2 m and 5 m, and height between 1 m and 1.8 m.

2.2 Objective function

The goal of this study is to maximize the insertion loss calculated at the receivers by changing the surface treatment on the barrier, described by the normalized admittance β. The 2D BEM, implemented in the software MICADO developed at the CSTB by Jean[10], has been used for this purpose. The BEM provides a way to calculate the complex pressure amplitude $p(R, f)$ at each frequency and at each receiver point, for a unit source amplitude. One can then define an average attenuation across all receivers at the frequency f_n:

$$A_n = \left[\frac{\sum_i |p(R_i, f_n)|^2}{\sum_i |p^{\text{in}}(R_i, f_n)|^2} \right]^{\frac{1}{2}} = \frac{P(f_n)}{P^{\text{in}}(f_n)} \tag{1}$$

where $p = p^{\text{in}} + p^{\text{sc}}$ is the total pressure field, p^{in} is the incident field independent of the scatterer and p^{sc} the scattered field. P is a RMS average pressure across the receivers and P^{in} the incident pressure which is a normalizing constant independent of the scattering surface. Then, from those attenuations at different frequencies, we consider a broadband attenuation based on the sound power levels L_w shown in Fig. 2. Defining an amplitude-like quantity $S = 10^{L_w/10}$ at all sixth-octave frequencies in the considered frequency range, the broadband attenuation is given by:

$$e = \frac{\sum_n S_n A_n^2}{\sum_n S_n} \tag{2}$$

which is equivalent to the objective function considered by Baulac et al.[1,2]. We would like to minimize the function e, which only depends on the admittance distribution once the geometry of the barrier is fixed (one can also calculate from the objective function a broadband insertion loss in dB(A) defined by $\text{IL} = -10 \log e$).

To carry on the optimization of the objective function, an iterative method based on the gradient has been chosen. Accurate calculation of the gradient is therefore necessary. In the following section, we derive a very simple expression which can then be used in a classical gradient-based optimization algorithm.

3 CALCULATION OF THE GRADIENT WITH RESPECT TO THE ADMITTANCE DISTRIBUTION

3.1 Notations

In order to define and to use the gradient with respect to the admittance distribution, which is a complex function defined on the surface of the barrier, we now introduce the concept of functional gradient. Let Γ be the planar curve defining the scattering surface (which is in fact the barrier and its image with respect to the side of the tramway). Let D be the set of piecewise continuous complex functions defined on Γ. The bracket notation $\langle ., . \rangle$ refers to the integral of the product of two functions in D. Let F be a complex functional defined on D. F is said to be differentiable in $f \in D$ if there exists a linear form L_f such that:

$$(\forall g \in D) \quad F(f + g) = F(f) + L_f(g) + o(\|g\|_\infty) \tag{3}$$

In this context, one can then identify the linear form L_f to a complex function $\mathrm{d}F/\mathrm{d}f$ (called the "gradient" or the "functional derivative" of F) such that:

$$(\forall g \in D) \quad L_f(g) = \left\langle \frac{\mathrm{d}F}{\mathrm{d}f}, g \right\rangle \tag{4}$$

Actually the function $\mathrm{d}F/\mathrm{d}f$ could be a generalized function and in this case the definition is to be taken in a distribution sense. Also, if a complex functional F is linear and has the form $F(f) = \langle f_0, f \rangle$ then the derivative is simply given by $\mathrm{d}F/\mathrm{d}f = f_0$. When the functional has several arguments, one can naturally use the notion of partial functional derivatives, written as $\partial F/\partial f$.

In the particular case when F takes real values, the gradient term $L_f(g)$ has to be real as well, and therefore it could be replaced by its real part in the definition (3). So, if F takes real values, it is equivalent to state that F is differentiable in f if there exists a complex function $\mathrm{d}F/\mathrm{d}f$ such that:

$$(\forall g \in D) \quad F(f+g) = F(f) + \mathrm{Re}\left\langle \frac{\mathrm{d}F}{\mathrm{d}f}, g \right\rangle + o(\,\|g\|_\infty\,) \tag{5}$$

Several properties of usual derivatives can be extended to the case of functional derivatives. For instance, for F a complex differentiable functional, one can also show that:

$$\left\langle \frac{\mathrm{d}|F|^2}{\mathrm{d}f}, g \right\rangle = F^* \left\langle \frac{\mathrm{d}F}{\mathrm{d}f}, g \right\rangle + F \left\langle \frac{\mathrm{d}F}{\mathrm{d}f}, g \right\rangle^* = \mathrm{Re}\left\langle 2\,F^* \frac{\mathrm{d}F}{\mathrm{d}f}, g \right\rangle \tag{6}$$

with * denoting complex conjugation. From this follows:

$$\frac{\mathrm{d}|F|^2}{\mathrm{d}f} = 2\,F^* \frac{\mathrm{d}F}{\mathrm{d}f} \quad \text{and} \quad \frac{\mathrm{d}|F|}{\mathrm{d}f} = \frac{F^*}{|F|} \frac{\mathrm{d}F}{\mathrm{d}f} \tag{7}$$

We now introduce the operators we will use in the resolution of the scattering problem satisfied by the pressure field. The problem is considered purely two-dimensional (the barrier is infinitely extended in one dimension), and is solved in the frequency domain so that the frequency f is fixed and $k = 2\pi f/c_0$ is the wavenumber. The time convention is $e^{-\mathrm{i}\omega t}$. Let $G(\mathbf{x}, \mathbf{y})$ be the Green's function of the Helmholtz equation. For a homogeneous atmosphere in presence of a rigid ground, the expression for G is:

$$G(\mathbf{x}, \mathbf{y}) = \frac{\mathrm{i}}{4}\left(H_0^{(1)}[k\sqrt{(y_1-x_1)^2+(y_2-x_2)^2}] + H_0^{(1)}[k\sqrt{(y_1-x_1)^2+(y_2+x_2)^2}]\right) \tag{8}$$

where $\mathbf{x} = (x_1, x_2)$ and $\mathbf{y} = (y_1, y_2)$ are two arbitrary points and $H_0^{(1)}$ is the Hankel function of order zero of the first kind. Given a function p on Γ, we then define the following operators[9]:

$$\begin{aligned} S\,p \;&:\; \mathbf{x} \mapsto \int_\Gamma G(\mathbf{x},\mathbf{y})\,p(\mathbf{y})\,\mathrm{d}\Gamma(\mathbf{y}) & D\,p \;&:\; \mathbf{x} \mapsto \int_\Gamma \frac{\partial G}{\partial n_2}(\mathbf{x},\mathbf{y})\,p(\mathbf{y})\,\mathrm{d}\Gamma(\mathbf{y}) \\ D^*p \;&:\; \mathbf{x} \mapsto \int_\Gamma \frac{\partial G}{\partial n_1}(\mathbf{x},\mathbf{y})\,p(\mathbf{y})\,\mathrm{d}\Gamma(\mathbf{y}) & N\,p \;&:\; \mathbf{x} \mapsto \int_\Gamma \frac{\partial^2 G}{\partial n_1\,\partial n_2}(\mathbf{x},\mathbf{y})\,p(\mathbf{y})\,\mathrm{d}\Gamma(\mathbf{y}) \end{aligned} \tag{9}$$

where the notation $\partial/\partial n_k$ refers to the normal derivative with respect to the k^{th} argument of a function. The expression for the operator N is simply formal under this form, but one can give a more rigorous definition of N in a variational context[10].

Since G is reciprocal, S and N are *self-adjoint* in the following sense: given two functions p and q defined on Γ, we have $\langle S\,p, q\rangle = \langle S\,q, p\rangle$ and $\langle Np, q\rangle = \langle Nq, p\rangle$. Moreover, D and D^* are adjoint of each other: $\langle Dp, q\rangle = \langle D^*q, p\rangle$. Finally, the notation $|_\Gamma$ refers to the fact that a function is evaluated on the scattering surface Γ.

3.2 Specifications of the scattering problem

Let Ω^e and Ω^i be the exterior and interior domains of the barrier. Considering a unit point source at (S), the total pressure p can be written as $p = p^{\text{in}} + p^{\text{sc}}$ where $p^{\text{in}}(\mathbf{x}) = G(S, \mathbf{x})$ is the field emitted by the source and the scattered field p^{sc} satisfies the problem:

$$\begin{cases} -(\nabla^2 + k^2)\, p^{\text{sc}} = 0 \ \text{ in } \Omega^e \\ \dfrac{\partial p^{\text{sc}}}{\partial n} + \mathrm{i}k\beta\, p^{\text{sc}} = h_1^{\text{in}}(\beta) \ \text{ on } \Gamma \qquad \text{with } \ h_1^{\text{in}}(\beta) = -\left.\dfrac{\partial p^{\text{in}}}{\partial n}\right|_\Gamma - \mathrm{i}k\beta\, p^{\text{in}}|_\Gamma \\ + \ \text{ radiation condition} \end{cases} \tag{10}$$

where β is the normalized admittance at the surface of the barrier and $h_1^{\text{in}}(\beta)$ corresponds to the influence of the incident field on the scatterer. The Kirchhoff-Helmholtz integral theorem states that the scattered field p^{sc} at the receiver point R_i is given by:

$$p^{\text{sc}}(R_i) = \int_\Gamma \Big(\frac{\partial G}{\partial n_2}(R_i, \mathbf{y}) + \mathrm{i}k\beta(\mathbf{y})\, G(R_i, \mathbf{y}) \Big)\, p_\Gamma(\mathbf{y})\, \mathrm{d}\Gamma(\mathbf{y}) \tag{11}$$

where p_Γ is the total pressure field on the scatterer, which we will call the *state*. It is well-known that p_Γ satisfies the equation:

$$\frac{1}{2}\, p_\Gamma - D p_\Gamma - S(\mathrm{i}k\beta p_\Gamma) = p^{\text{in}}|_\Gamma \tag{12}$$

The term $1/2$ implies that the curve Γ is sufficiently smooth (which is not a restrictive assumption in a variational context[10]). However, taken by itself, this equation does not admit a unique solution for all values of the wavenumber. To partially avoid this problem, following the approach used by Jean[10], which is a variation on the Burton and Miller's approach[11], one can show that p_Γ also satisfies the following equation:

$$N p_\Gamma + D^*(\mathrm{i}k\beta p_\Gamma) + \mathrm{i}k\beta\, D p_\Gamma + \mathrm{i}k\beta\, S(\mathrm{i}k\beta p_\Gamma) = h_1^{\text{in}}(\beta) \tag{13}$$

One can show that this equation has a unique solution provided that $\mathrm{Re}\,\beta$ is nonzero everywhere. This is the equation used, under its variational form, in the BEM software MICADO when the admittance on the ground is uniform. We will refer to Eqn. (13) as the *state* equation.

3.3 Lagrangian and rewriting of the gradient expression

As stated earlier, to achieve the minimization of the objective function, its gradient is needed. Here we consider the minimization of the root mean square (RMS) pressure P at one particular frequency as a function of the admittance β. P depends directly on β and p_Γ through the scattered field expression given in Eqn. (11). But, through the state equation, the state p_Γ is an implicit function of β and therefore it is uneasy to obtain directly an expression for the gradient of P. To avoid this problem, we introduce the Lagrangian $\mathcal{L}$ defined for three generic functions $\hat{\beta}$, $\hat{p}_\Gamma$ and $\hat{q}_\Gamma$:

$$\begin{cases} \mathcal{L}(\hat{\beta}, \hat{p}_\Gamma, \hat{q}_\Gamma) = P(\hat{\beta}, \hat{p}_\Gamma) + Q(\hat{\beta}, \hat{p}_\Gamma, \hat{q}_\Gamma) \\ \text{with } \ Q(\hat{\beta}, \hat{p}_\Gamma, \hat{q}_\Gamma) = \mathrm{Re}\,\langle N\hat{p}_\Gamma + D^*(\mathrm{i}k\hat{\beta}\hat{p}_\Gamma) + \mathrm{i}k\hat{\beta}\, D\hat{p}_\Gamma + \mathrm{i}k\hat{\beta}\, S(\mathrm{i}k\hat{\beta}\hat{p}_\Gamma) - h_1^{\text{in}}(\hat{\beta}), \hat{q}_\Gamma \rangle \end{cases} \tag{14}$$

The term Q has been chosen so that it satisfies the property $Q(\beta, p_\Gamma, \hat{q}_\Gamma) = 0$ for any function $\hat{q}_\Gamma$, which implies:

$$(\forall \hat{q}_\Gamma \in D) \ \ P(\beta, p_\Gamma) = \mathcal{L}(\beta, p_\Gamma, \hat{q}_\Gamma) \tag{15}$$

We then introduce the adjoint state q_Γ so that the Lagrangian is stationary at $(\beta, p_\Gamma, q_\Gamma)$:

$$\frac{\partial \mathcal{L}}{\partial q_\Gamma}(\beta, p_\Gamma, q_\Gamma) = 0 \tag{16}$$

$$\frac{\partial \mathcal{L}}{\partial p_\Gamma}(\beta, p_\Gamma, q_\Gamma) = 0 \quad \Longleftrightarrow \quad \frac{\partial Q}{\partial p_\Gamma}(\beta, p_\Gamma, q_\Gamma) = -\frac{\partial P}{\partial p_\Gamma}(\beta, p_\Gamma) \tag{17}$$

Equation (16) is simply the state equation satisfied by p_Γ. Equation (17) is a new equation satisfied by q_Γ and will be referred to as the *adjoint state* equation. If we were interested in directly finding what the optimal admittance is, we would also impose the stationarity with respect to β, but this equation is too difficult to solve directly, which is why we use a gradient-based iterative minimization. We use here the Lagrangian to get a simple expression for the gradient.

Since p_Γ depends on β but not $\hat{q}_\Gamma$, taking the total derivative with respect to β of Eqn. (15) yields:

$$(\forall \hat{q}_\Gamma \in D) \;\; \frac{\mathrm{d}P}{\mathrm{d}\beta}(\beta, p_\Gamma) = \frac{\partial \mathcal{L}}{\partial \beta}(\beta, p_\Gamma, \hat{q}_\Gamma) + \frac{\partial \mathcal{L}}{\partial p_\Gamma}(\beta, p_\Gamma, \hat{q}_\Gamma) \frac{\mathrm{d}p_\Gamma}{\mathrm{d}\beta} \tag{18}$$

In particular, taking $\hat{q}_\Gamma = q_\Gamma$ and recalling Eqn.(17) yields:

$$\frac{\mathrm{d}P}{\mathrm{d}\beta}(\beta, p_\Gamma) = \frac{\partial \mathcal{L}}{\partial \beta}(\beta, p_\Gamma, q_\Gamma) = \frac{\partial P}{\partial \beta}(\beta, p_\Gamma) + \frac{\partial Q}{\partial \beta}(\beta, p_\Gamma, q_\Gamma) \tag{19}$$

The total derivative has therefore been replaced by a partial derivative, which means that one can avoid dealing with the implicit dependence due to the state equation.

3.4 Adjoint state equation

Here we derive the explicit expression of Eqn. (17). Using Eqn. (7) and (11), the derivative of P with respect to p_Γ is:

$$\frac{\partial P}{\partial p_\Gamma} = \sum_i \frac{p(R_i)^*}{P} \frac{\partial p^{\mathrm{sc}}(R_i)}{\partial p_\Gamma} = \sum_i \frac{p(R_i)^*}{P} \Big(\frac{\partial G}{\partial n_2}(R_i, .) + \mathrm{i}k\beta\, G(R_i, .) \Big) \stackrel{\mathrm{def}}{=} -h_2^{\mathrm{in}}(\beta, p_\Gamma) \tag{20}$$

since p^{in} does not depend on p_Γ. h_2^{in} depends on p_Γ through the scattered field components in $p(R_i)$. For the derivative of Q, using adjoint properties of the different operators, one can rewrite Q as:

$$Q(\hat{\beta}, \hat{p}_\Gamma, \hat{q}_\Gamma) = \mathrm{Re}\, \langle N\hat{q}_\Gamma + \mathrm{i}k\hat{\beta}\, D\hat{q}_\Gamma + D^*(\mathrm{i}k\hat{\beta}\hat{q}_\Gamma) + \mathrm{i}k\hat{\beta}\, S\,(\mathrm{i}k\hat{\beta}\hat{q}_\Gamma), \hat{p}_\Gamma \rangle - \mathrm{Re}\, \langle h_1^{\mathrm{in}}(\hat{\beta}), \hat{q}_\Gamma \rangle \tag{21}$$

We recognize the expression of the form $\mathrm{Re}\, \langle \partial Q/\partial p_\Gamma, \hat{p}_\Gamma \rangle$ plus a constant of p_Γ where:

$$\frac{\partial Q}{\partial p_\Gamma} = N\hat{q}_\Gamma + \mathrm{i}k\hat{\beta}\, D\hat{q}_\Gamma + D^*(\mathrm{i}k\hat{\beta}\, \hat{q}_\Gamma) + \mathrm{i}k\hat{\beta}\, S\,(\mathrm{i}k\hat{\beta}\hat{q}_\Gamma) \tag{22}$$

Using Eqn. (20) and (22), Eqn. (17) becomes:

$$Nq_\Gamma + \mathrm{i}k\beta\, Dq_\Gamma + D^*(\mathrm{i}k\beta q_\Gamma) + \mathrm{i}k\beta\, S\,(\mathrm{i}k\beta q_\Gamma) = h_2^{\mathrm{in}}(\beta, p_\Gamma) \tag{23}$$

The adjoint state equation (Eqn. (23)) has therefore exactly the same form than the state equation (Eqn. (13)) with a different right-hand side. In fact, one can show that the adjoint state is the distribution of pressure on the barrier due to the radiation of weighted point sources at the receivers locations. Writing down Eqn. (12) for this related scattering problem yields:

$$\frac{1}{2}\, q_\Gamma - Dq_\Gamma - S\,(\mathrm{i}k\beta q_\Gamma) = q^{\mathrm{in}}|_\Gamma \qquad \text{with} \quad q^{\mathrm{in}}(\mathbf{x}) = \sum_i \frac{p(R_i)^*}{P}\, G(R_i, \mathbf{x}) \tag{24}$$

3.5 Expression of the gradient

Finally, we give the explicit expression of Eqn. (19). Recalling Eqn. (11), we have:

$$\frac{\partial P}{\partial \beta} = \sum_i \frac{p(R_i)^*}{P} \frac{\partial p^{\mathrm{sc}}(R_i)}{\partial \beta} = \mathrm{i}k p_\Gamma \sum_i \frac{p(R_i)^*}{P} G(R_i, .) = \mathrm{i}k p_\Gamma \, q^{\mathrm{in}}|_\Gamma \tag{25}$$

by the definition of q^{in}. As before, using adjoint properties of the integral operators, the term Q can be rewritten as a quadratic function of β. Its derivative is given by:

$$\frac{\partial Q}{\partial \beta}(\beta, p_\Gamma, q_\Gamma) = \mathrm{i}k \left[p_\Gamma \, D q_\Gamma + q_\Gamma \, D p_\Gamma + p^{\mathrm{in}}|_\Gamma \, q_\Gamma + p_\Gamma \, S(\mathrm{i}k\beta q_\Gamma) + q_\Gamma \, S(\mathrm{i}k\beta p_\Gamma) \right] \tag{26}$$

Recalling Eqn. (12) and (24), this simplifies to:

$$\frac{\partial Q}{\partial \beta}(\beta, p_\Gamma, q_\Gamma) = \mathrm{i}k \left[p_\Gamma \, q_\Gamma - p_\Gamma \, q^{\mathrm{in}}|_\Gamma \right] \tag{27}$$

so that Eqn. (19) is simply given by:

$$\frac{\mathrm{d}P}{\mathrm{d}\beta} = \mathrm{i}k \, p_\Gamma \, q_\Gamma \tag{28}$$

Therefore, calculation of the gradient of the attenuation with respect to the admittance can be achieved by the following steps:

- calculate p_Γ by solving the state equation (Eqn. (13)), which depends only on β
- calculate the total pressure field at the receivers $p(R_i)$ based on p_Γ and β, using Eqn. (11)
- calculate q_Γ by solving the adjoint state equation (Eqn. (23)), which depends on β and $p(R_i)$
- calculate the total gradient of P from Eqn. (28), which depends on p_Γ and q_Γ

This process has been validated against the semi-analytical expression one can obtain in the case of a semi-cylindrical barrier[5].

3.6 Gradient of the broadband objective function

If the distribution of admittance β can be related to a small number of parameters a_m, using the chain rule, the total derivative of the RMS pressure P with respect to the parameter a_m is given by:

$$\frac{\mathrm{d}P}{\mathrm{d}a_m} = \frac{\mathrm{d}P}{\mathrm{d}\beta} \circ \frac{\mathrm{d}\beta}{\mathrm{d}a_m} = \mathrm{Re}\left\langle \mathrm{i}k \, p_\Gamma \, q_\Gamma, \frac{\mathrm{d}\beta}{\mathrm{d}a_m} \right\rangle \tag{29}$$

Also, we can use this to calculate the gradient of the objective function defined in section 2. Recalling Eqn. (2) the derivative of e with respect to a parameter a_m is:

$$\frac{\mathrm{d}e}{\mathrm{d}a_m} = \frac{1}{\sum_n S_n} \sum_n S_n \, \frac{2\,P(f_n)}{P^{\mathrm{in}}(f_n)^2} \, \frac{\mathrm{d}P(f_n)}{\mathrm{d}a_m} \tag{30}$$

with $\mathrm{d}P(f_n)/\mathrm{d}a_m$ calculated using Eqn (29).

We are now able to calculate the gradient of the objective function with respect to the parameters describing the admittance. For each frequency, one only needs to know the state and

the adjoint state, which is achieved by solving two classical BEM integral equations per frequency. The main advantage of using the adjoint state is, once the state and the adjoint state are known, the calculation of the gradient with respect to a parameter is fast (it is simply an integral), and therefore a great number of parameters can be used without significant increase of computation time. Also, the expression of the gradient is simply a post-treatment of the BEM calculations, and therefore its calculation does not require coding a new integral equation solver.

4 APPLICATION: OPTIMIZATION OF POROUS AND MICRO-PERFORATED PANELS

As an example of application, we propose to optimize the admittance when the barrier is covered by a finite number of panels. The variables to optimize are then the parameters describing the admittance of each panel as well as the width of each panel.

We consider two types of panels usually used in noise control: micro-perforated panels (MPP) and porous layers, which can be used to model vegetation layers. A MPP typically absorbs sound in selected frequency bands, which can be more or less broad depending on the hole radius. A porous layer, typically described by the Delany & Bazley model, provides reasonable broadband absorption but is more efficient at high frequencies. The layer version of this model has been shown to model many grass-like surfaces relatively accurately[12].

4.1 Admittance models

4.1.1 Micro-perforated panel

The impedance of a MPP can be written in terms of four parameters: the porosity s, the hole radius a_0, the thickness of the panel l_0 and the cavity depth D. The normalized impedance can then be written in the $\mathrm{e}^{-\mathrm{i}\omega t}$ convention as[13]:

$$z_{\mathrm{MPP}}(f) = -\mathrm{i}\,\frac{kl_0}{s}\left(\frac{1}{\Theta(x')} + \frac{16}{3\pi}\,\frac{a_0}{l_0}\,\frac{\Psi(\xi)}{\Theta(x)}\right) + \mathrm{i}\cot(kD) \quad \text{with} \quad \Theta(w) = 1 - \frac{2}{w\sqrt{\mathrm{i}}}\,\frac{J_1(w\sqrt{\mathrm{i}})}{J_0(w\sqrt{\mathrm{i}})} \tag{31}$$

$k = 2\pi f/c_0$ is the wavenumber, $\xi = \sqrt{s}$, $x/a_0 = \sqrt{2\pi f\rho_0/\mu}$ and $x'/a_0 = \sqrt{2\pi f\rho_0/\mu'}$ are the so-called perforate constants, μ is the viscosity and $\mu' \approx 2.2\,\mu$ represents equivalent thermal effects. The normalized admittance is then simply $\gamma_{\mathrm{MPP}}(f) = 1/z_{\mathrm{MPP}}(f)$. Also, in order to treat the MPP as locally reacting, the back cavity should be partitioned in small cells[13].

4.1.2 Rigid-backed Delany and Bazley model

Here we consider a layer of porous material of depth d ended by a rigid backing. Following Delany and Bazley[14], the normalized impedance $\tilde{z}$ and complex wavenumber $\tilde{k}$ only depend on one parameter σ and are given by:

$$\begin{cases} \tilde{z}(f) = 1 + 0.0511\,(\sigma/f)^{0.75} + \mathrm{i}\,0.0768\,(\sigma/f)^{0.73} \\ \tilde{k}/k = 1 + 0.0858\,(\sigma/f)^{0.7} + \mathrm{i}\,0.175\,(\sigma/f)^{0.59} \end{cases} \tag{32}$$

However, due to the finite depth d of the layer and assuming a rigid backing, the normalized impedance becomes $z_{\mathrm{DB}}(f) = \tilde{z}(f)\,\coth(-\mathrm{i}\tilde{k}d)$ and therefore the admittance is $\gamma_{\mathrm{DB}}(f) = 1/z_{\mathrm{DB}}(f)$.

4.2 Description of the optimization problem

We consider three geometries for the barrier: square, thin wall and T-shape (see Fig. 3). Each straight segment of the barrier is assumed to be covered by one or several MPP or porous layers, or is assumed to be rigid on the part of the barrier far from the source (where the admittance has been shown not to influence the attenuation significantly[5]).

The chosen optimization algorithm is the Sequential Quadratic Programming (SQP) algorithm, which consists in iteratively approximating and minimizing the objective function as a quadratic function of the parameters. Furthermore, to allow a better search of the design space, five random starting points are used. To completely define the optimization problem, we still need to choose a range for the admittance parameters, which depends on the type of parameter:

- **MPP**. Porosity: $s \in [0.01, 0.4]$; hole radius: $a_0 \in [0.5, 5]\,\text{mm}$; panel thickness: $l_0 \in [0.2, 1]\,\text{cm}$; cavity depth $D \in [1, 10]\,\text{cm}$
- **Porous layer**. Flow resistivity: $\sigma \in [50, 200]\,\text{kPa s/m}^2$; layer depth: $d \in [1, 10]\,\text{cm}$

The choice of those ranges is based on physically feasible values. Specifically, the range of flow resistivities has been chosen according to grassland-type soils values determined by Attenborough et al.[12].

4.3 Results

Each run of the optimization algorithm converged within less than one hundred iterations. Broadband insertion losses obtained for the best optimized solutions and for the case of a purely absorbent (covered everywhere with a porous layer of flow resistivity $\sigma = 50\,\text{kPa s/m}^2$ and thickness $d = 10\,\text{cm}$) or rigid barrier are shown in Table 1. Corresponding third-octave insertion losses and optimized panel arrangements for each geometry are shown in Fig. 4.

First, one can notice that the rigid barriers provide a relatively low attenuation in the considered frequency range, which could be explained by the multiple reflections happening between the tramway side and the barrier. Absorbing treatment on the barrier surface attenuates those reflections and therefore enhances the insertion loss by about 10 dB(A). Using absorbing porous-like materials is therefore necessary for the good performance of the barrier. However, using an optimized arrangement of absorbing panels and MPPs can further increase the performance, especially for the T-shape geometry (improvement of 6 dB(A)). Third-octave insertion losses (see Fig. 4) show that the optimized panel arrangement and especially the presence of the resonant panels can increase the attenuation in the mid-frequency range (500 to 1200 Hz), which is where the source has the most spectral content, therefore providing a significant increase in the broadband insertion loss.

5 CONCLUSION

The 2D BEM coupled with a simple optimization algorithm has been used in order to design the admittance of a low-height tramway noise barrier. The gradient of the attenuation with respect to the admittance at each frequency can be obtained efficiently using the adjoint state approach, which allows to avoid dealing with the implicit dependence of the pressure distribution on the barrier on the admittance and to use many parameters without significant increase of the computation time. Also, the gradient can be expressed as a post-treatment of the BEM and therefore can be computed with the results of any commercial BEM software. Besides,

several simplifying assumptions have been made to make the calculations faster in the iterative optimization process (2D approximation, rigid ground, tramway side as a vertical baffle).

This method has been applied to three classical geometries for a low-height barrier: square, thin wall and T-shape. The barrier is assumed to be covered with several porous layers and MPPs, and the optimization is used in order to automatically tune the parameters of each panel. First, in this configuration, the T-shape geometry seems to be the most efficient compared to the two other ones, which is in agreement with many studies on noise barriers.

Also, results suggest that treating the barrier close to the source with an absorbing material decreases the negative effects of the multiple reflections happening between the barrier and the tramway providing a significant improvement on the insertion loss of 10 dB(A). Besides, an optimized arrangement of porous panels and MPPs can yield an extra improvement up to 6 dB(A), due to an increase of attenuation in the mid-frequency range, thanks to the presence of the resonant panels. The optimization process we developed therefore provides a convenient way to choose admittance distribution parameters in order to attenuate the noise in the most sensitive frequency range, and could be used in the design stage of a new noise barrier.

ACKNOWLEDGMENTS

The authors would like to thank the French Ministry of Ecology, Sustainable Development, Transport and Housing (MEDDTL) for the financial support of this work.

REFERENCES

[1] M. Baulac, J. Defrance, P. Jean, "Optimization of low height noise protections in urban areas", In *Forum Acousticum 2005, Budapest*, 1075-1080.

[2] M. Baulac, J. Defrance, P. Jean, F. Minard, "Efficiency of noise protections in urban areas: prediction and scale model measurements", *Acta Acust. United Ac.* **92**, 530-539 (2006)

[3] P. J. Thorsson, "Optimisation of low-height noise barriers using the equivalent sources method", *Acta Acust.* **86**, 811-820 (2000)

[4] P. J. Thorsson, "Combined effects of admittance optimisation on both barrier and ground", *Appl. Acoust.* **64**, 693-711 (2003)

[5] A. Jolibois, D. Duhamel, V. W. Sparrow, J. Defrance, P. Jean, "Scattering by a cylinder covered with an arbitrary distribution of impedance and application to the optimization of a tramway noise abatement system", *J. Sound. Vib.* (submitted)

[6] M. A. Pallas, J. Lelong, R. Chatagnon, "Characterization of tram noise emission and contribution of the noise sources", *Appl. Acoust.* **72**, 437-450 (2011)

[7] G. Allaire, "Conception optimale des structures" (optimal design of structures), *Springer* (2007)

[8] D. Duhamel, "Efficient calculation of the three-dimensional sound pressure field around a noise barrier", *J. Sound Vib.* **197**, 547-571 (1996)

[9] I. Terrasse, T. Abboud, "Modélisation des phénomènes de propagation d'ondes" (Modeling of wave propagation phenomena), *Ecole Polytechnique* (2007)

[10] P. Jean, "A variational approach for the study of outdoor sound propagation and application to railway noise", *J. Sound Vib.* **212**(2), 275-294 (1998)

[11] A. J. Burton, J. F. Miller, "The Application of Integral Equation Methods to the Numerical Solution of Some Exterior Boundary-Value Problems", *Proceedings of the Royal Society of London* **323** (1553), 201-210 (1971)

[12] K. Attenborough, I. Bashir, S. Taherzadeh, "Outdoor ground impedance models", *J. Acoust. Soc. Am.* **129**(5), 2806-2819 (2011)

[13] F. Asdrubali, G. Pispola, "Properties of transparent sound-absorbing panels for use in noise barriers", *J. Acoust. Soc. Am.* **121**(1), 214-221 (2007)

[14] M. E. Delany, E. N. Bazley, "Acoustical properties of fibrous absorbent materials", *Appl. Acoust.* **3**, 105-116 (1970)

Table 1 - Comparison of broadband insertion losses in dB(A) for the optimized solution and reference cases (rigid barrier and absorbent barrier) for the three considered geometries.

	Thin wall	Square	T-shape
Rigid	3.7	3.1	5.6
Absorbent	14.3	15.7	16.6
Opt. sol.	17.8	21.6	23.1

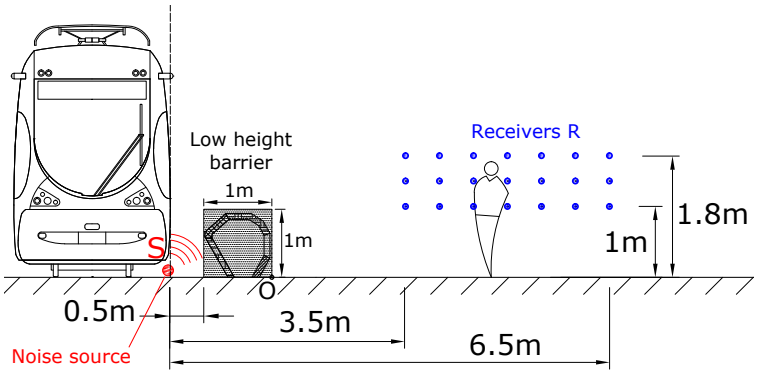

Fig. 1 - Implementation of the low-height barrier close to the tramway and definitions of the source and receivers locations. The dotted line corresponds to the idealization of the tramway side as a vertical baffle.

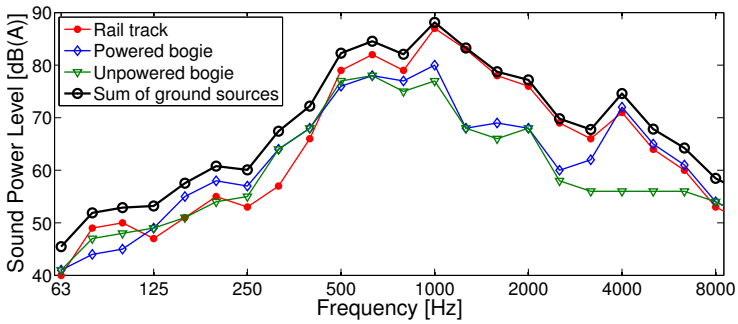

Fig. 2 - Comparison of third octave spectra of the different sources identified by Pallas et al.[6] and their incoherent summation.

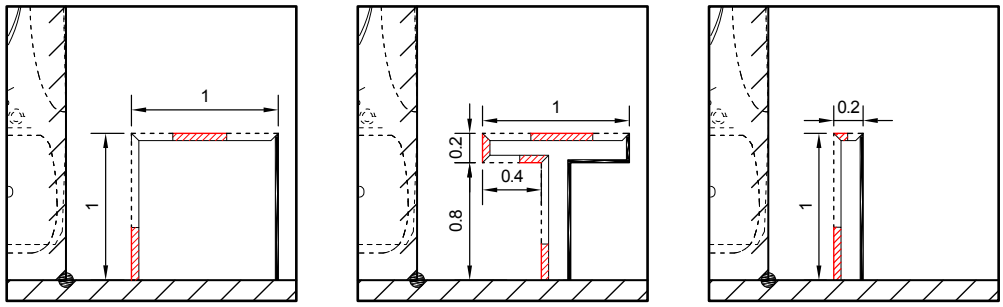

Fig. 3 - Definition of the three considered geometries for the low-height barrier and generic arrangement of panels (red hatch: porous layer - dotted black line: MPP - thick black line: rigid). Dimensions are in meters.

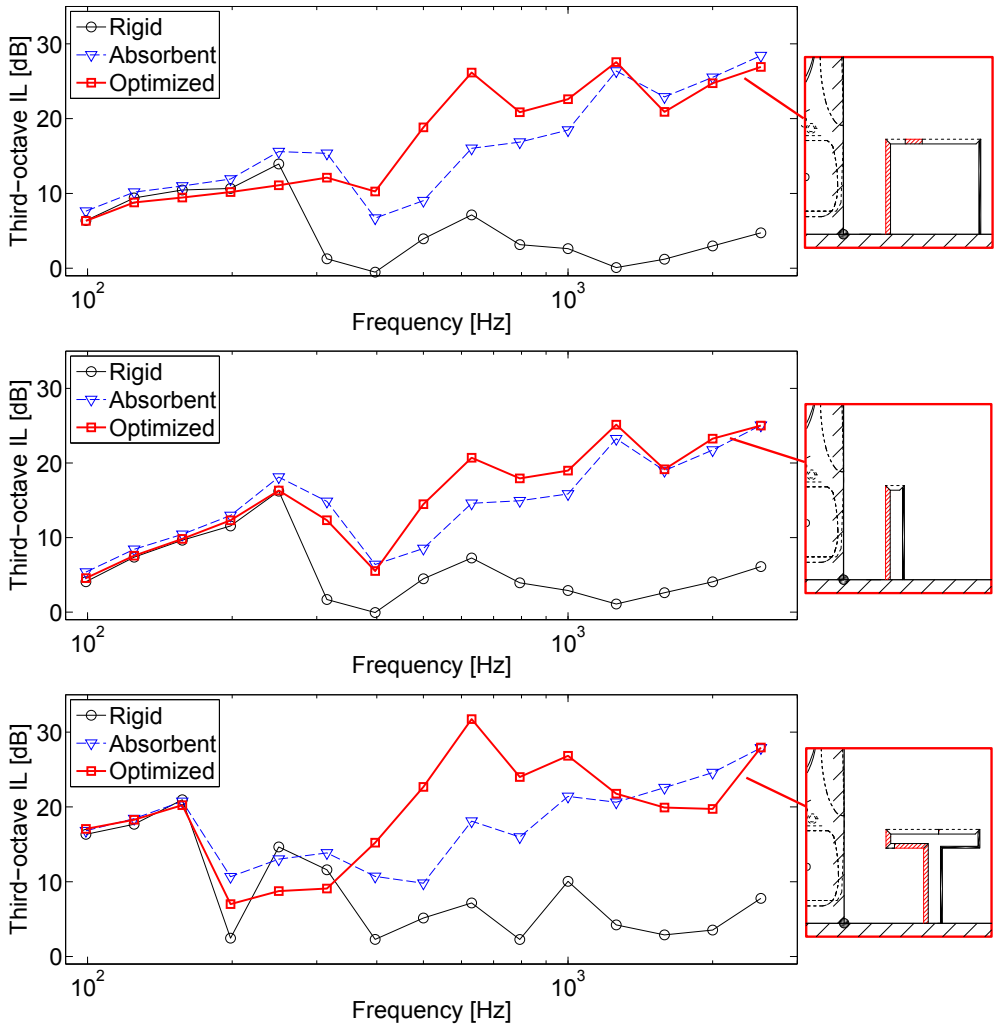

Fig. 4 - Comparison of third-octave insertion losses for for three geometries and for three admittance distributions: uniformly rigid (thin black line), uniformly porous (thin dotted blue line) and optimized arrangement of MPPs and porous layers (thick red line). Top: square - middle: thin wall - bottom: T-shape. The optimized arrangement for each geometry is also shown.